Key Points:
- Ozone depleting substances are a major driver of Brewer-Dobson circulation trends
- Emission of these substances has been phased out by the Montreal Protocol
- That phasing out will result in considerably reduced BDC trends in the 21st century

Significant Weakening of Brewer-Dobson Circulation Trends Over the 21st Century as a Consequence of the Montreal Protocol

Lorenzo M. Polvani[1,2,3] [ID], **Marta Abalos**[3,4] [ID], **Rolando Garcia**[3] [ID], **Doug Kinnison**[3] [ID], and **William J. Randel**[3] [ID]

[1]Department of Applied Physics and Applied Mathematics, Columbia University, New York, NY, USA, [2]Lamont Doherty Earth Observatory, Columbia University, Palisades, NY, USA, [3]National Center for Atmospheric Research, Boulder, CO, USA, [4]Departamento Física de la Tierra y Astrofísica, Universidad Complutense de Madrid, Madrid, Spain

Abstract It is well established that increasing greenhouse gases, notably CO_2, will cause an acceleration of the stratospheric Brewer-Dobson circulation (BDC) by the end of this century. We here present compelling new evidence that ozone depleting substances are also key drivers of BDC trends. We do so by analyzing and contrasting small ensembles of "single-forcing" integrations with a stratosphere resolving atmospheric model with interactive chemistry, coupled to fully interactive ocean, land, and sea ice components. First, confirming previous work, we show that increasing concentrations of ozone depleting substances have contributed a large fraction of the BDC trends in the late twentieth century. Second, we show that the phasing out of ozone depleting substances in coming decades—as a consequence of the Montreal Protocol—will cause a considerable reduction in BDC trends until the ozone hole is completely healed, toward the end of the 21st century.

1. Introduction

Originally postulated to exist in order to explain the observed spatial distributions of stratospheric ozone (Dobson, 1956; Dobson et al., 1929) and water vapor (Brewer, 1949), the Brewer-Dobson circulation (hereafter, BDC) is now recognized as being central to our understanding of how air parcels and trace gases are transported within the stratosphere (Butchart, 2014; Plumb, 2002; Shepherd, 2007), and how they are exchanged between the stratosphere and the troposphere (Holton, 1990). Understanding how and why the BDC might change in a changing climate is thus of paramount importance.

At present, one very robust modeling result has been established: increasing concentrations of well-mixed greenhouse gases (GHG) will cause a considerable acceleration of the BDC over the 21st century. First reported by Rind et al. (1990), this result has been confirmed in many single-model studies (e.g., Butchart and Scaife, 2001; Garcia and Randel, 2008), as well as the multimodel projections of several model intercomparison projects (Butchart et al., 2006, 2010, Hardiman et al., 2014). Increasing GHG, however, are not the sole anthropogenic forcing affecting the BDC. Evidence has been mounting that another anthropogenic forcing, ozone depleting substances (ODS), may actually be of crucial importance for understanding BDC trends.

In a recent paper Polvani et al. (2017) have argued, on the basis of both observational and modeling evidence, that ODS have been a major driver of tropical upwelling and BDC trends over the last two decades of the twentieth century. This conclusion is supported by several earlier modeling studies, starting from a hint in the last paragraph of Austin and Li (2006). For instance, Oman et al. (2009) find that increasing ODS are the most important forcing that causes age of air (AoA) to decrease from 1960 to 2004 in their model. Or again, contrasting time slice integrations for the years 1960 and 2000, Oberländer-Hayn et al. (2015) conclude that ODS cause half the BDC changes over that period in their model. More importantly, the recent observational study of Fu et al. (2015) found a strong hemispheric asymmetry in the dynamically driven tropical lower-stratospheric temperatures trends since 1979 and noted that the bulk of the signal is linked to the Southern Hemisphere. Since GHG are well mixed, this clearly implicates the ozone hole, and therefore ODS, as key drivers of tropical upwelling and BDC trends.

Whereas GHG concentrations have been steadily increasing and are expected to keep increasing in coming decades, ODS trends are not monotonic in time. Recall that ODS concentrations were growing rapidly in the second half of the twentieth century but have started to decline since the late 1990s as a consequence of the signing and implementation of the Montreal Protocol (and its amendments). This raises an interesting question: if increasing ODS have been responsible for a large fraction of the BDC acceleration up to the late 1990s, what are the implications of the Montreal Protocol for BDC trends in the 21st century?

We answer that question in this paper using small ensembles of single-forcing integrations with a state-of-the-art stratosphere-resolving, chemistry-coupled model. We find that the reduction in ODS concentrations in coming decades, and the accompanying closing of the ozone hole over the South Pole, causes a significant reduction in BDC trends from the present to the year 2080. Furthermore, we show here that the fingerprint of ODS on BDC trends is very robust and is easily seen in the seasonal and hemispheric asymmetries in these trends, and in their clear differences between the 20th century and the 21st century.

2. Methods

The model. In this paper we use the Community Earth System Model (version 1) with the Whole Atmosphere Community Climate Model (WACCM) as the atmospheric component. WACCM includes an interactive atmospheric chemistry package and is coupled to fully interactive ocean, land, and sea ice component. The horizontal resolution of WACCM is 1.9° in latitude and 2.5° in longitude; its vertical resolution ranges about 1.2 km near the tropopause, to about 2 km near the stratopause, with the model top located near 140 km (and a total of 66 levels). The baseline version of our model is detailed in Marsh et al. (2013), with later improvements to stratospheric heterogeneous chemistry (which produce an accurate simulation of the ozone hole, as documented by Solomon et al., 2015) and to orographic gravity wave forcing (as documented by Garcia et al., 2017).

The integrations. Here we analyze three small ensembles of WACCM integrations spanning the period 1960–2100. Each ensemble is composed of three members, with minutely different initial conditions but identical forcings (as in Kay et al., 2015), taken from one of the scenarios proposed by the International Global Atmospheric Chemistry/Stratosphere-troposphere Processes and their Role in Climate (IGAC/SPARC) Chemistry-Climate Model Initiative (CCMI, Morgenstern et al., 2017). The first ensemble is forced as per the specifications of scenario REF-C2: in a nutshell, these integrations follow the World Meteorological Organization (WMO) (2011) A1 scenario for ODS (WMO, 2011), and the RCP 6.0 for the other GHG, tropospheric ozone precursors and aerosol emissions (Meinshausen et al., 2011). For the second ensemble the forcings are nearly identical, except for ODS, which do not evolve in time and are fixed at 1960 levels, as per scenario SEN-C2-fODS of CCMI. The third ensemble is forced with the SEN-C2-fGHG scenario of CCMI: here the GHG (i.e., CH_4, N_2O, and CO_2) are held fixed at 1960 values, and all other forcings are as in REF-C2. For simplicity and clarity, we will refer to these three ensembles with the labels All forcings, Fixed ODS, and Fixed GHG, respectively.

3. Results

We start by recalling the nonmonotonic nature of the ODS forcing, as this is crucial for understanding the differences in BDC trends between the 20th and 21st centuries. In Figure 1a we show the time series of equivalent effective stratospheric chlorine (EESC) in our All forcings integrations (computed as in Newman et al., 2009). Notice how EESC, which represents the amount of halogens from ODS emissions that have been advected into the stratosphere and are responsible for ozone loss there, peaks around the year 2000, about a decade after the emissions of ODS start being phased out by the Montreal Protocol, and then decreases continuously over the 21st century. In contrast, CO_2 and N_2O mixing ratios (see Figure 1b) increase monotonically over the entire 1960–2100 period, and CH_4 also increases monotonically until approximately 2070 (in the RCP 6.0 scenario chosen by the CCMI).

Although ODS are greenhouse gases and thus cause some surface warming (Velders et al., 2007), their primary and most dramatic effect to date has been the chemical destruction of stratospheric ozone in the late twentieth century, notably over the South Pole. This is shown in Figure 1c: the red curves, for the October time series of southern polar cap ozone as simulated in our All forcings runs, indicate a 50% loss by the year 2000, and a clear reversal of trends thereafter, as the ozone hole heals. We emphasize that the impact of ODS on polar stratospheric ozone is strongly seasonal: it is confined to the spring season (contrast the October and March curves). Similar, but much weaker, springtime ozone trends are found over the northern polar cap,
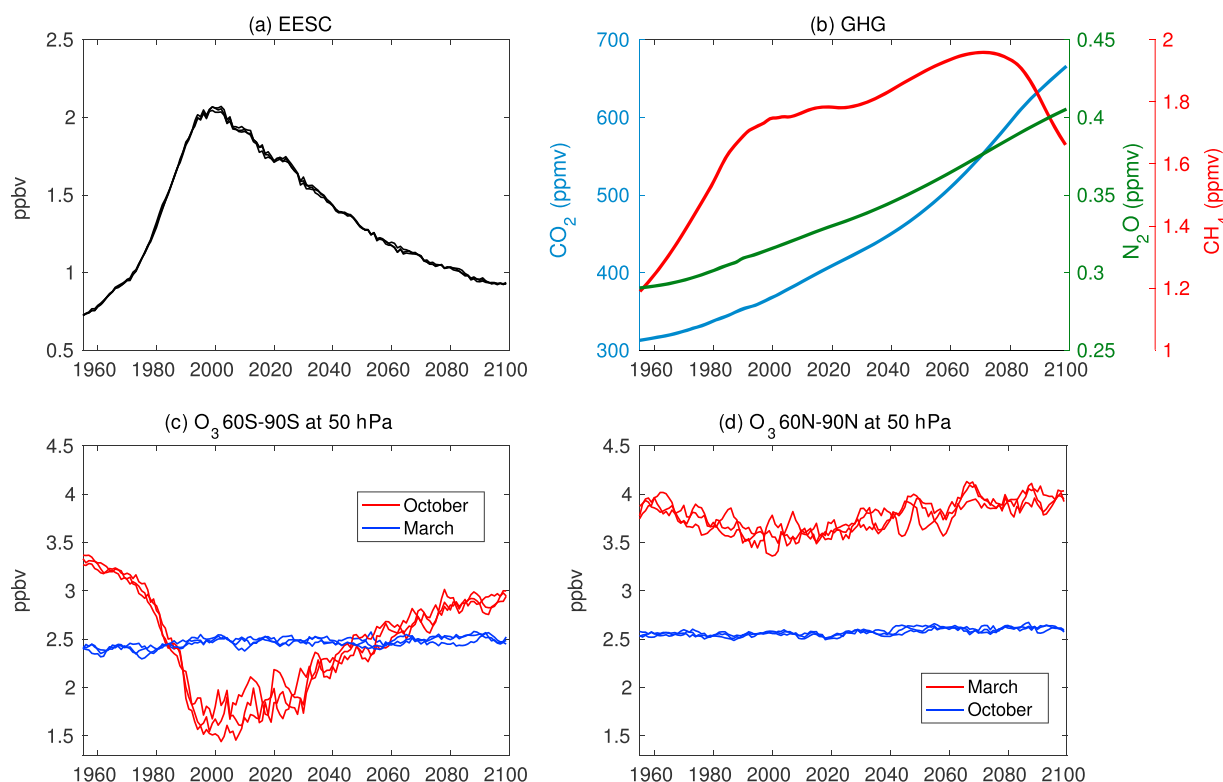
Figure 1. Time series of (a) equivalent effective stratospheric chlorine (EESC); (b) greenhouse gases; (c and d) 50 hPa polar cap ozone averaged 60–90°S and 60–90°N, respectively. In Figures 1a, 1c, and 1d we plot three curves of each color, one for each member of our All forcings ensemble, and each curves is slightly smoothed with a five-point running mean. In Figure 1a, the EESC values are computed at 50 hPa. In Figure 1b, the colored curves illustrate the prescribed global mean surface abundances of the major well-mixed greenhouse gases, as indicated by the labels on the ordinate axes. In Figures 1a and 1b annual means are shown; in Figures 1c and 1d the two key spring/fall months are shown in red/blue, respectively, as per the legend in those panels.

of the order of 10% at this level in March (Figure 1d). This large hemispheric asymmetry, and the strongly seasonal character of stratospheric ozone trends, will provide clear fingerprints of the effect of ODS—via stratospheric ozone—on the BDC.

Given the nonmonotonicity of ozone/ODS curves presented in Figure 1, it clearly makes no sense to look at changes and compute linear trends over the entire 1960–2100 period. We thus confine the analysis to two subperiods: the first from 1965 to 2000, and the second from 2000 to 2080, which we refer to as "the past" and "the future", respectively, throughout the remainder of this paper. While our runs start in 1960, it takes a few years for the age-of-air tracer to reach equilibrium: this is why we select 1965 as the starting point for the past. We choose to terminate the future period at 2080 to avoid complications from the methane trend reversal, and also because the ozone curves appear to be basically flat after that year. It will be clear that our key results are insensitive to the specific choices of start and end years.

With those two key periods defined, we are now ready to discuss past and future BDC trends, and the relative importance of ODS and GHG. We start by analyzing the age-of-air (AoA) tracer, which provides an integral measure of the stratospheric transport circulation, accounting for both the slow meridional/vertical overturning and the fast quasi-horizontal eddy mixing (Garcia et al., 2011; Hall & Plumb, 1994; Waugh & Hall, 2002). Past and future AoA trends for the ensemble mean of our three All forcings integrations are shown in Figures 2a and 2b, respectively. Contrasting these two panels, it is immediately clear that future trends are much weaker than past trends. Averaged from 70 hPa to 1 hPa, our model shows that global and annual mean AoA trends are 4 times smaller in the future than in the past. This is the first key finding of our study: our model projects a very substantial reduction of BDC trends in the coming decades.

We now ask the following: what is the cause of the future reduction in BDC trends? The answer is easily guessed from Figure 1: only one anthropogenic forcing reverses sign between the past and the future. This points
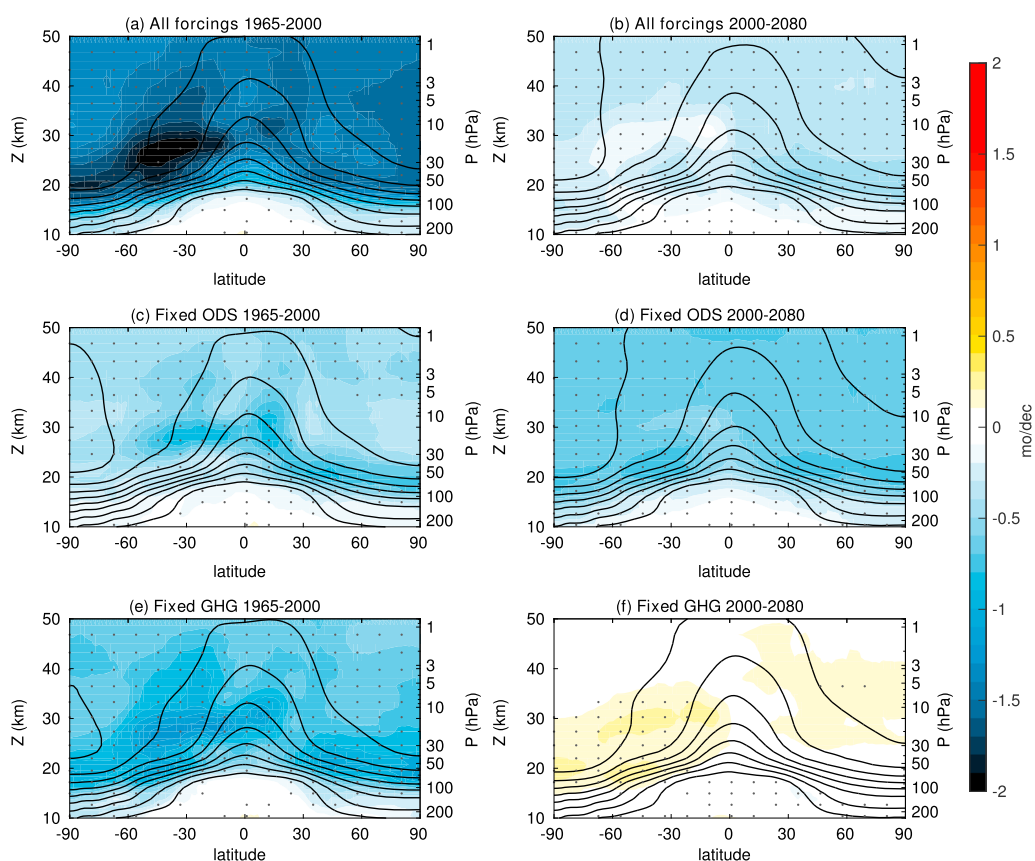
Figure 2. Annual and zonal mean age of air (AoA) trends in color, superimposed on AoA climatology (black contours). (a, b) All forcings integrations. (c, d) Fixed ODS integrations. (e, f) Fixed GHG integrations. Past trends (1965–2000) (Figures 2a, 2c, and 2e). Future trends (2000–2080) (Figures 2b, 2d, and 2f). The climatology is computed by averaging the years 1965–2000 for Figures 2a, 2c, and 2e, and 2000–2080 for Figures 2b, 2d, and 2f, using the ensemble mean of the corresponding integrations, as is contoured using an interval of 6 months, starting with that value in the lower stratosphere and increasing monotonically with height. For the trends, in colors, the contour interval is 0.1 months/decade. Dotted regions indicate statistically significant trends at the 95% confidence level.

to ODS, therefore, as the likely anthropogenic forcing responsible for the considerable weakening of future BDC trends. The key role of ODS on the BDC is confirmed in the remaining panels of Figure 2, where past and future AoA trends are shown for the Fixed ODS (Figures 2c and 2d) and Fixed GHG integrations (Figures 2e and 2f).

Consider first the past BDC trends. Contrasting Figures 2c and 2e, one can see that past trends for the Fixed GHG runs are considerably larger than for the Fixed ODS runs, by a factor of 1.5 in our model. This confirms the conclusion reached by Polvani et al. (2017) with a different model, namely, that increasing ODS have been a crucial driver of BDC acceleration in the last few decades. The novelty here consists in realizing that in the future, the BDC trends caused by ODS will reverse sign, and this will lead to a dramatic slowdown in BDC acceleration. This is easily seen in Figures 2d and 2f and constitutes the second key finding our paper that the significant reduction in BDC trends in the 21st century is a consequence of the Montreal Protocol, which is directly responsible for the decline of ODS concentrations.

To better illustrate this, the entire 1965–2080 time series of global and annual mean AoA, at 10 and 70 hPa, is shown in Figure 3. The large impact of ODS can be seen at both levels, indicating that both shallow and deep branches (Birner & Bönisch, 2011; Hardiman et al., 2014) of the BDC are affected by ODS, their impact being larger at higher levels. Focus first on the Fixed ODS runs (red curves) and see how the monotonically increasing GHG cause only a monotonic reduction in AoA, from 1965 all the way to 2080. When the ODS forcing is added (blue curves) the AoA trends become much stronger from 1965 to 2000, and much weaker
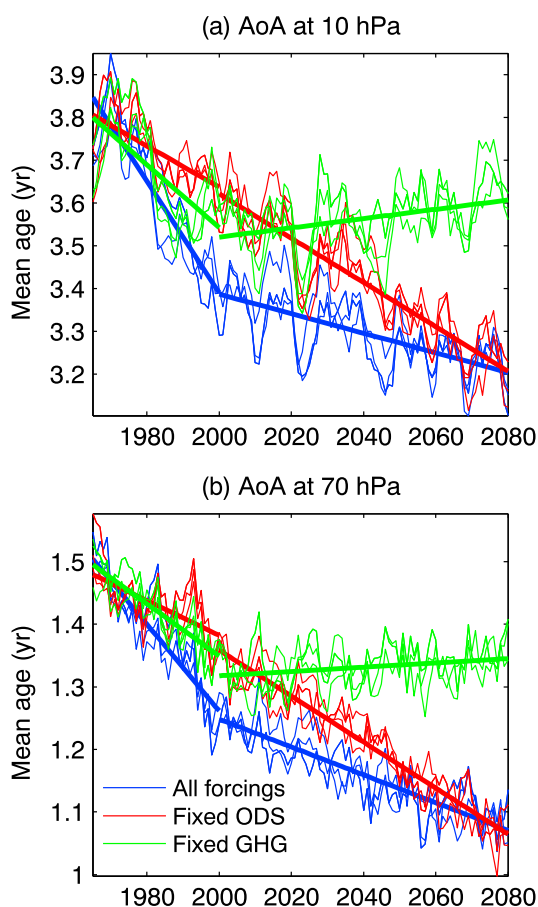
(a) AoA at 10 hPa

(b) AoA at 70 hPa

Figure 3. Annual and global mean AoA at (a) 10 hPa and (b) 70 hPa. Blue: All forcings. Red: Fixed ODS. Green: Fixed GHG. For clarity, the yearly values have been smoothed with a three-point running mean. Straight lines show linear fits to the ensemble means, for the past and the future: all trends are statistically significant at the 95% level.

from 2000 to 2080. The fact that ODS accelerate the BDC in the past and decelerate it in the future is visually captured by the V-shaped green curves, showing the Fixed GHG runs. The values of the fitted trend lines, for both past and future, can be found in supporting information Table S1. Note that additivity between the Fixed GHG and Fixed ODS runs is not expected, as forcings beyond GHG and ODS (e.g., aerosols) are present in the All forcings runs. However, the trends in Table S1 are approximately additive: from this we deduce that GHG and ODS are the largest drivers of BDC trends and that nonlinearities are small.

One might now ask via what mechanism ODS are able to affect the BDC. The answer is relatively simple: apart from their direct radiative effect as greehouse gases, ODS primarily impact the BDC via ozone depletion/recovery: this is easily deduced from the hemispheric asymmetry and strong seasonality of past and future BDC trends. Consider the time series of the residual-mean vertical velocity w^* (defined, e.g., in equations (4) and (5) of Butchart, 2014) at 70 hPa, plotted for the polar caps and the tropics in Figure 4 (for completeness, supporting information Figure S1 shows similar quantities, but using turnaround latitudes to illustrate the entire overturning circulation). Let us start by focusing on the top row which shows the annual mean southern polar cap, tropical average, and northern polar cap w^* time series — from left to right — for the different WACCM runs we are analyzing. One clearly sees that the largest separation between the red and blue curves is found over the South Pole: this indicates that the impact of ODS on w^* occurs primarily as a consequence of the ozone hole, which forms from 1965 to 2000 and closes by 2080 (approximately). Note also that the green and blue curves are almost identical over the southern polar cap (Figure 4a): since keeping GHG fixed has little effect on w^*, we conclude that nearly all past and future trends are forced by ODS in that region.

The key role of the ozone hole on the BDC is further corroborated by the very strong seasonality of the w^* trends. Contrasting the December–February (DJ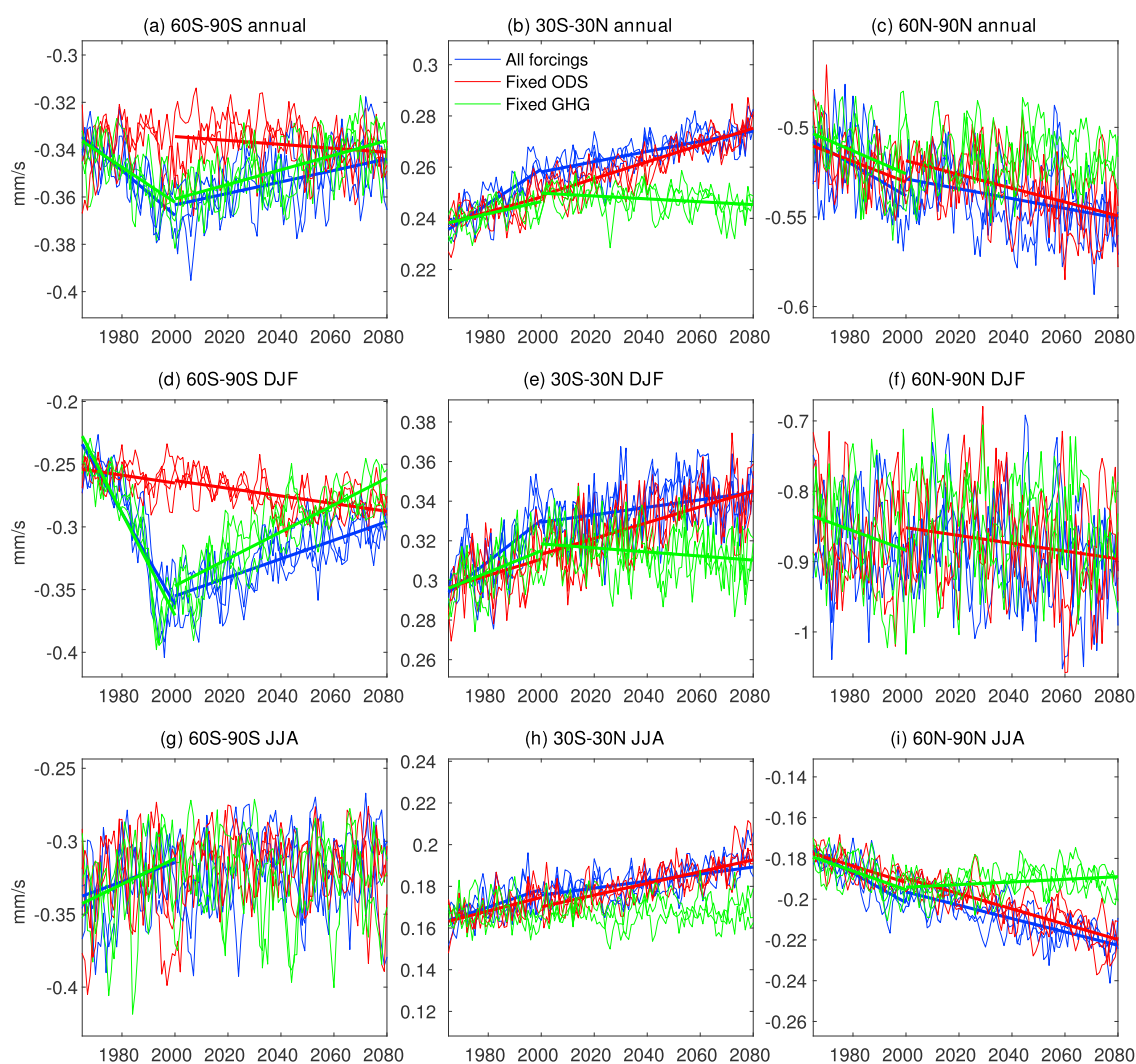F) time series in Figures 4d–4f to the June–August (JJA) time series in Figures 4g–4i, one can immediately see that the signal is almost entirely confined to the summer months over the southern polar cap (Figure 4d) (for completeness, the remaining seasons are shown in supporting information Figure S2). The red and blue curves are most clearly separated in Figures 4a and 4d, indicating that ODS affect the BDC primarily via the ozone hole. So while the impact of ODS on the BDC (via the ozone hole) is present in only one hemisphere and one season, its amplitude is large enough to be reflected in substantial AoA trend differences in the annual mean and in both hemispheres, as already noted in Figure 2.

It may not be immediately obvious why the largest impact of ODS on the BDC should be found in austral summer, since the peak ozone depletion over the South Pole is found in the spring. This has to do with dynamical nature of the BDC, which is driven by waves which break and deposit momentum in the stratosphere. As shown in numerous previous studies (e.g., Polvani et al., 2011; Son et al., 2008), the atmospheric circulation changes induced by ODS occur in DJF lagged by a couple of months with respect to the largest (October) ozone anomalies. While not fully understood at a fundamental level, this lag is very robust and is found in both models and observation (see, e.g., Figure 2 of Thompson et al., 2011), resulting in DJF being the season when the effect of ozone depletion on the circulation manifest themselves.

Finally, to leave no doubt as to the robustness of our key findings, we present Ψ^* trends at all latitudes and heights, for both the past and the future, and for all three ensembles: Ψ^* is the residual-mean stream function (in the Transformed Eulerian Mean formalism of Andrews and McIntyre, 1978, of which w^* is the latitudinal derivative) and gives a full picture of the residual-mean stratospheric circulation. We focus on DJF, to best bring

Figure 4. Time series of the residual vertical velocity w^* at 70 hPa for the All forcings (blue), Fixed ODS (red), and Fixed GHG (green) integrations. (a–c) Annual mean. (d–f) DJF. (g–i) JJA. Polar cap average, from 60 to 90°S (Figures 4a, 4d, and 4g) and 60 to 90°N (Figures 4c, 4f, and 4i). Tropical average (30S–30°N) (Figures 4b, 4e, and 4h). Straight lines are drawn, for past or future, where trends are statistically significant at the 95% level, as computed from linear fits to the ensemble means.

out the ODS signal: Ψ^* trends for that season are shown Figure 5. For completeness, however, the annual Ψ^* trends can be found in supporting information Figure S3: since the ODS impact is large, all the key features in Figure 5 are also seen in the annual mean, albeit with a reduced amplitude.

The layout of Figure 5 is identical to the one in Figure 2, so let us first consider the top row, which shows the ensemble mean of the three All forcings integrations, and contrast past and future changes. For the past (Figure 5a) the blue/red dipole straddling the equator indicates that the BDC is accelerating in both hemispheres in the twentieth century. In the 21 century (Figure 5b), however, the future trends reverse in the Southern Hemisphere (from blue to red): this indicates a future deceleration of the BDC in that hemisphere in that season. Second, in agreement with previous studies, we find that GHG cause a future acceleration in Ψ^* in both hemispheres, for both the past and the future (Figures 5c and 5d). Third, and most importantly, in the Southern Hemisphere ODS cause a stronger acceleration in the past and a stronger deceleration in the future (Figures 5e and 5f) than GHG. Note that while the effect of ODS on the BDC is largely confined to one season and one hemisphere, its amplitude is so large that it is clearly seen in the annual and global AoA trends, as shown in Figures 2 and 3.
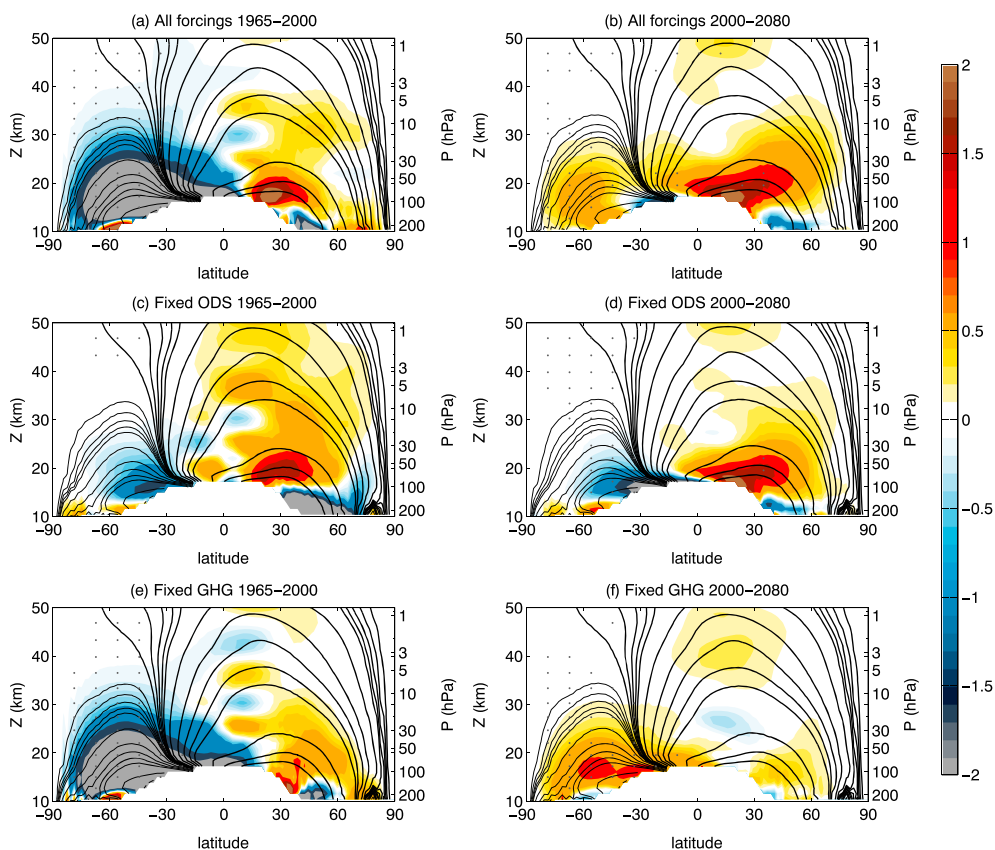
Figure 5. As in Figure 1 but for Ψ* in DJF. Black contour values for the climatology are ± {1, 2, … , 5, 10, 20, … , 50, 100, 150, 200 } kg/m/s, with the negative contours plotted thinner than the positive contours. Color contours for the trends are ± {0.1, 0.2, … , 0.5, 1, 1.5, 2 } kg/m/s/decade.

4. Discussion

Careful analysis of small ensembles of single-forcing model integrations has revealed that ODS are a major forcing of BDC trends. This fact is not widely appreciated at present: for instance, the most recent review paper on the subject (Butchart, 2014) makes no mention of ODS and discusses GHG as the sole cause of BDC acceleration. However, several recent studies, reviewed in section 1, strongly suggest that ODS have played a major role in the acceleration of the BDC over the second half of the twentieth century: we have here provided new modeling confirmation of that role. Furthermore, and this is the novel finding of this study, we have shown that the phasing out of ODS, as mandated by the Montreal Protocol, will cause significantly reduced BDC trends in coming decades.

Our model integrations show that stratospherically averaged age-of-air trends from 2000 to 2080 will be 4 times smaller than they have been from 1965 to 2000, and a big part of that considerable reduction comes from the fact that ODS have contributed more than half of the trends up to the year 2000. Needless to say, the specific values of past and future trends are likely to be dependent on scenario and model used, and therefore, our quantitative results will need to be compared to those of other models and scenarios. Preliminary analysis of nearly a dozen models participating in the CCMI and the older Chemistry-Climate Model Validation Activity (CCMVal) Phase 2 project (Eyring et al., 2008) is showing that our results are highly robust, and we plan to report on that in an separate upcoming paper.

Given the robust and easily understood trends in our model integrations, one might wonder why it has proven so difficult to detect BDC trends in the observations (see the introduction of Abalos et al., 2015, for an updated discussion). First, it is important to keep in mind that the BDC cannot be measured directly but needs to be indirectly inferred. Second, using ensembles of model integrations, we can distinguish the forced signal from

the large internal variability (Hardiman et al., 2017), but it is not easy to do so from observations. Third, the observational period (which starts at 1979) is relatively short, and nearly all studies to date—failing to appreciate the importance of ODS for the BDC—have computed a single linear trend across the entire period, thus canceling a larger 20th century signal with a weaker signal in the early 21st century.

Be that as it may, our study suggests a new, simple, yet powerful observable for validating the impact of ODS on the stratospheric circulation: the interhemispheric asymmetry in AoA and BDC trends. For the past, that asymmetry is already apparent, both in models (see Figure 2a above) and in observations (see Figure 2a of Ploeger et al., 2015, for instance). For the future, we expect the asymmetry to reverse: the closing of the ozone hole in Southern Hemisphere will cause trends to be weaker there than in the Northern Hemisphere, as our integrations clearly show (see Figure 2b).

References

Abalos, M., Legras, B., Ploeger, F., & Randel, W. (2015). Evaluating the advective Brewer-Dobson circulation in three reanalyses for the period 1979–2012. *Journal of Geophysical Research: Atmospheres*, *120*, 7534–7554. https://doi.org/10.1002/2015JD023182

Andrews, D., & McIntyre, M. (1978). Generalized Eliassen-Palm and Charney-Drazin theorems for waves on axisymmetric mean flows in compressible atmospheres. *Journal of the Atmospheric Sciences*, *35*(2), 175–185.

Austin, J., & Li, F. (2006). On the relationship between the strength of the Brewer-Dobson circulation and the age of stratospheric air. *Geophysical Research Letters*, *33*, L17807. https://doi.org/10.1029/2006GL026867

Birner, T., & Bönisch, H. (2011). Residual circulation trajectories and transit times into the extratropical lowermost stratosphere. *Atmospheric Chemistry and Physics*, *11*(2), 817–827.

Brewer, A. W. (1949). Evidence for a world circulation provided by the measurements of helium and water vapour distribution in the stratosphere. *Quarterly Journal of the Royal Meteorological Society*, *75*(326), 351–363.

Butchart, N. (2014). The Brewer-Dobson circulation. *Reviews of Geophysics*, *52*(2), 157–184. https://doi.org/10.1002/2013RG000448

Butchart, N., & Scaife, A. A. (2001). Removal of chlorofluorocarbons by increased mass exchange between the stratosphere and troposphere in a changing climate. *Nature*, *410*(6830), 799–802.

Butchart, N., Scaife, A., Bourqui, M., De Grandpré, J., Hare, S., Kettleborough, J., ... Sigmond M (2006). Simulations of anthropogenic change in the strength of the Brewer-Dobson circulation. *Climate Dynamics*, *27*(7–8), 727–741.

Butchart, N., Cionni, I., Eyring, V., Shepherd, T., Waugh, D., Akiyoshi, H., ... Tian W (2010). Chemistry–climate model simulations of twenty-first century stratospheric climate and circulation changes. *Journal of Climate*, *23*(20), 5349–5374.

Dobson, G. (1956). Origin and distribution of the polyatomic molecules in the atmosphere. *Proceedings of the Royal Society of London. Series A, Mathematical and Physical Sciences*, *236*(1205), 187–193.

Dobson, G. M., Harrison, D., & Lawrence, J. (1929). Measurements of the amount of ozone in the Earth's atmosphere and its relation to other geophysical conditions. Part III. *Proceedings of the Royal Society of London. Series A, Containing Papers of a Mathematical and Physical Character*, *122*(790), 456–486.

Eyring, V., Chipperfield, M. P., Giorgetta, M. A., Kinnison, D. E., Matthes, K., Newman, P. A., ... Waugh, D. W. (2008). Overview of the new CCMval, reference and sensitivity simulations in support of upcoming ozone and climate assessments and the planned SPARC CCMVal report, SPARC Newslet, *30*, 20–26.

Fu, Q., Lin, P., Solomon, S., & Hartmann, D. L. (2015). Observational evidence of strengthening of the Brewer-Dobson circulation since 1980. *Journal of Geophysical Research: Atmospheres*, *120*, 10,214–10,228. https://doi.org/10.1002/2015JD023657

Garcia, R. R., & Randel, W. J. (2008). Acceleration of the Brewer-Dobson circulation due to increases in greenhouse gases. *Journal of the Atmospheric Sciences*, *65*(8), 2731–2739.

Garcia, R. R., Randel, W. J., & Kinnison, D. E. (2011). On the determination of age of air trends from atmospheric trace species. *Journal of the Atmospheric Sciences*, *68*(1), 139–154.

Garcia, R. R., Smith, A. K., Kinnison, D. E., Cámara, Á.d. l., & Murphy, D. J. (2017). Modification of the gravity wave parameterization in the Whole Atmosphere Community Climate Model: Motivation and results. *Journal of the Atmospheric Sciences*, *74*(1), 275–291.

Hall, T. M., & Plumb, R. A. (1994). Age as a diagnostic of stratospheric transport. *Journal of Geophysical Research*, *99*(D1), 1059–1070.

Hardiman, S. C., Butchart, N., & Calvo, N. (2014). The morphology of the Brewer-Dobson circulation and its response to climate change in CMIP5 simulations. *Journal of the Royal Meteorological Society*, *140*(683), 1958–1965.

Hardiman, S. C., Lin, P., Scaife, A. A., Dunstone, N. J., & Ren, H.-L. (2017). The influence of dynamical variability on the observed Brewer-Dobson circulation trend. *Geophysical Research Letters*, *44*, 2885–2892. https://doi.org/10.1002/2017GL072706

Holton, J. (1990). On the global exchange of mass between the stratosphere and troposphere. *Journal of the Atmospheric Sciences*, *47*(3), 392–395.

Kay, J., Deser, C., Phillips, A., Mai, A., Hannay, C., Strand, G., ... Vertenstein, M. (2015). The Community Earth System Model (CESM) large ensemble project: A community resource for studying climate change in the presence of internal climate variability. *Bulletin of the American Meteorological Society*, *96*, 1333–1349.

Marsh, D. R., Mills, M. J., Kinnison, D. E., Lamarque, J.-F., Calvo, N., & Polvani, L. M. (2013). Climate change from 1850 to 2005 simulated in CESM1 (WACCM). *Journal of Climate*, *26*(19), 7372–7391.

Meinshausen, M., Smith, S. J., Calvin, K., Daniel, J. S., Kainuma, M., Lamarque, J., ... van Vuuren, D. (2011). The RCP greenhouse gas concentrations and their extensions from 1765 to 2300. *Climatic change*, *109*(1–2), 213–241.

Morgenstern, O., Hegglin, M. I., Rozanov, E., O'Connor, F. M., Abraham, N. L., Akiyoshi, H., ... Zeng, G. (2017). Review of the global models used within Phase 1 of the Chemistry-Climate Model Initiative (CCMI). *Geoscientific Model Development*, *10*(2), 639–671.

Newman, P. A., Oman, L. D., Douglass, A. R., Fleming, E. L., Frith, S. M., Hurwitz, M. M., ... Velders, G. J. M. (2009). What would have happened to the ozone layer if chlorofluorocarbons (CFCs) had not been regulated? *Atmospheric Chemistry and Physics*, *9*, 2113–2128.

Oberländer-Hayn, S., Meul, S., Langematz, U., Abalichin, J., & Haenel, F. (2015). A chemistry-climate model study of past changes in the Brewer-Dobson circulation. *Journal of Geophysical Research: Atmospheres*, *120*, 6742–6757. https://doi.org/10.1002/2014JD022843

Oman, L., Waugh, D. W., Pawson, S., Stolarski, R. S., & Newman, P. A. (2009). On the influence of anthropogenic forcings on changes in the stratospheric mean age. *Journal of Geophysical Research*, *114*, D03105. https://doi.org/10.1029/2008JD010378

Ploeger, F., Abalos, M., Birner, T., Konopka, P., Legras, B., Müller, R., & Riese, M. (2015). Quantifying the effects of mixing and residual circulation on trends of stratospheric mean age of air. *Geophysical Research Letters*, *42*(6), 2047–2054.

Plumb, R. A. (2002). Stratospheric transport. *Journal of the Meteorological Society of Japan. Ser. II*, *80*(4B), 793–809.

Polvani, L. M., Waugh, D. W., Correa, G. J., & Son, S.-W. (2011). Stratospheric ozone depletion: The main driver of twentieth-century atmospheric circulation changes in the Southern Hemisphere. *Journal of Climate*, *24*, 795–812.

Polvani, L. M., Wang, L., Aquila, V., & Waugh, D. W. (2017). The impact of ozone-depleting substances on tropical upwelling, as revealed by the absence of lower-stratospheric cooling since the late 1990s. *Journal of Climate*, *30*(7), 2523–2534.

Rind, D., Suozzo, R., Balachandran, N., & Prather, M. (1990). Climate change and the middle atmosphere. Part I: The doubled CO_2 climate. *Journal of the Atmospheric Sciences*, *47*(4), 475–494.

Shepherd, T. G. (2007). Transport in the middle atmosphere. *Journal of the Meteorological Society of Japan. Ser. II*, *85B*, 165–191.

Solomon, S., Kinnison, D., Bandoro, J., & Garcia, R. (2015). Simulation of polar ozone depletion: An update. *Journal of Geophysical Research: Atmospheres*, *120*, 7958–7974. https://doi.org/10.1002/2015JD023365

Son, S.-W., Polvani, L., Waugh, D., Akiyoshi, H., Garcia, R., Kinnison, D., . . . Shibata, K. (2008). The impact of stratospheric ozone recovery on the Southern Hemisphere westerly jet. *Science*, *320*(5882), 1486–1489.

Thompson, D. W., Solomon, S., Kushner, P. J., England, M. H., Grise, K. M., & Karoly, D. J. (2011). Signatures of the Antarctic ozone hole in Southern Hemisphere surface climate change. *Nature Geoscience*, *4*(11), 741–749.

Velders, G., Andersen, S., Daniel, J., Fahey, D., & McFarland, M. (2007). The importance of the Montreal protocol in protecting climate. *Proceedings of the National Academy of Sciences of the United States of America*, *104*, 4814–1819.

Waugh, D., & Hall, T. (2002). Age of stratospheric air: Theory, observations, and models. *Reviews of Geophysics*, *40*(4), 1010. https://doi.org/10.1029/2000RG000101

World Meteorological Organization (WMO) (2011). Scientific Assessment of Ozone Depletion: 2010. Global Ozone Research 399 and Monitoring Project-Report No. 52. Geneva, Switzerland.